

Calculation of the Linear-Absorption Spectrum of an Ideal Two-Dimensional System of MoS₂

Vo Chau Duc Phuong ¹

Supervisors

Dr. Huynh Thanh Duc ²

¹University of Science, Ho Chi Minh city

²Institute of Applied Mechanics and Informatics

14/07/2024

Outline

- 1 Overview
- 2 Method
 - Three-band Tight-binding Model
 - Semiconductor Bloch Equations
 - Inter-band Polarization
- 3 Numerical Results
- 4 Summary and Outlook

Transition Metal Dichalcogenides Monolayers

Group VI-B Transition Metal Dichalcogenides (TMD) are compound semiconductors of the type MX_2 . :

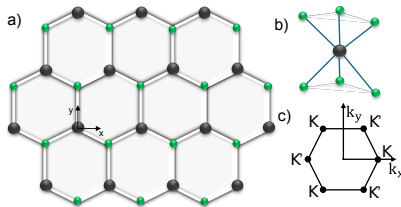


Figure: Structure of TMD and its first Brillouin Zone. M is Transition Metal atom (black dots), X is Dichalcogenide atom (green dots)

Transition Metal Dichalcogenide Monolayers

Properties

- They are stable in both mono- and few-layer in the air at room temperature.
- They are semiconductors with a direct band gap in visible light range.
- Their crystal structure has no center of inversion.
- Strong spin-orbit coupling (SOC) in TMD monolayers leads to spin splitting of hundreds meV.

⇒ Promising materials in electronic and optoelectronic applications (for example: solar cells with energy conversion efficiency surpassing the Shockley-Queisser limit).

Exciton Binding Energy In TMD

Exciton binding energy can be extracted from the linear absorption spectrum

Overview

- TMD is a low-dimensional material → huge exciton binding energy in compared with bulk semiconductors → electron-hole Coulomb interaction need to be calculated and taken into account.
- Early theories predict large binding energy (0.5 – 1 eV) in compare with experiment (0.2 – 0.5 eV) ⇒ more precise calculations to match with the experiments.
- Theories only fit bandstructure around highly symmetry points such as K/K' , not on entire BZ ⇒ a models for fitting in the entire BZ.

Tight-binding (TB) wave function has the form:

$$|\psi_{\lambda\mathbf{k}}(\mathbf{r})\rangle = \sum_{\alpha} c_{\lambda\alpha}(\mathbf{k}) \sum_{\mathbf{R}} e^{i\mathbf{k}\mathbf{R}} |\phi_{\alpha}(\mathbf{r} - \mathbf{R})\rangle. \quad (1)$$

The Time-independence Schrödinger equation:

$$H_{1e} \sum_{\alpha} c_{\lambda\alpha}(\mathbf{k}) \sum_{\mathbf{R}} e^{i\mathbf{k}\mathbf{R}} |\phi_{\alpha}(\mathbf{r} - \mathbf{R})\rangle = \varepsilon_{\lambda}(\mathbf{k}) \sum_{\alpha} c_{\lambda\alpha}(\mathbf{k}) \sum_{\mathbf{R}} e^{i\mathbf{k}\mathbf{R}} |\phi_{\alpha}(\mathbf{r} - \mathbf{R})\rangle.$$

Multiply with $\langle\phi_{\beta}|$ on the left and take integral over \mathbf{r}

$$\sum_{\alpha} [H_{\beta\alpha}^{TB}(\mathbf{k}) - \varepsilon_{\lambda}(\mathbf{k})\delta_{\beta\alpha}] c_{\lambda\alpha}(\mathbf{k}) = 0. \quad (2)$$

Tight-binding Hamiltonian matrix elements:

$$H_{\beta\alpha}^{TB}(\mathbf{k}) = \sum_{\mathbf{R}} \langle\phi_{\beta}(\mathbf{r})| H_{1e} |\phi_{\alpha}(\mathbf{r} - \mathbf{R})\rangle. \quad (3)$$

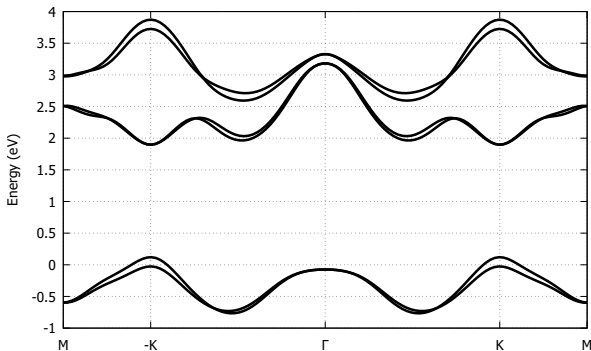
Use basic functions of d-type orbitals:

$$|\phi_1\rangle = d_{z^2}, |\phi_2\rangle = d_{xy}, |\phi_3\rangle = d_{x^2-y^2}.$$

Three-band TB Hamiltonian with SOC has the form:

$$H_{6\times 6}^{TB}(\mathbf{k}) = \begin{bmatrix} H_{3\times 3}^{TB}(\mathbf{k}) + \gamma L_z & 0 \\ 0 & H_{3\times 3}^{TB}(\mathbf{k}) - \gamma L_z \end{bmatrix}, \quad L_z = \begin{bmatrix} 0 & 0 & 0 \\ 0 & 0 & i \\ 0 & -i & 0 \end{bmatrix}.$$

Figure: Band structure of MoS_2 monolayer¹



¹Liu et al., "Three-band tight-binding model for monolayers of group-VIB transition metal dichalcogenides".

Multiband semiconductor Bloch equations (SBE) with Coulomb interaction in Hatree Fock approximation:

$$\begin{aligned} \frac{d}{dt} \rho_{\lambda\lambda'}(\mathbf{k}, t) = & -\frac{i}{\hbar} (\varepsilon_{\lambda}(\mathbf{k}) - \varepsilon_{\lambda'}(\mathbf{k})) \rho_{\lambda\lambda'}(\mathbf{k}) \\ & - i \sum_{\mu} (\Omega_{\lambda\mu}(\mathbf{k}) \rho_{\mu\lambda'}(\mathbf{k}, t) - \rho_{\lambda\mu}(\mathbf{k}, t) \Omega_{\mu\lambda'}(\mathbf{k})) \\ & + \frac{\rho_{\lambda\lambda'}(\mathbf{k}, t)}{T_2} (1 - \delta_{\lambda\lambda'}), \end{aligned} \quad (4)$$

where

$$\Omega_{\mu\nu}(\mathbf{k}) = \frac{1}{\hbar} \left(\frac{e}{m} \mathbf{A}(t) \mathbf{p}_{\mu\nu}(\mathbf{k}) - \sum_{\alpha\beta\mathbf{q}} W_{\mathbf{k},\mathbf{k}+\mathbf{q},\mathbf{q}}^{\alpha\mu\beta\nu} \rho_{\beta\alpha}(\mathbf{k} + \mathbf{q}) \right), \quad (5)$$

$$\mathbf{p}_{\mu\nu}(\mathbf{k}) = \frac{m}{\hbar} \sum_{\alpha,\beta} c_{\mu\alpha}^*(\mathbf{k}) \nabla_{\mathbf{k}} H_{\alpha\beta}^{TB}(\mathbf{k}) c_{\nu\beta}(\mathbf{k}), \quad (6)$$

$$W_{\mathbf{k}\mathbf{k}'\mathbf{q}}^{\alpha\beta\gamma\delta} = \frac{e^2}{2\epsilon_0\epsilon_{\infty}} \frac{1}{|\mathbf{q}|} \sum_{\mu,\nu} c_{\alpha\mu}^*(\mathbf{k} + \mathbf{q}) c_{\delta\mu}(\mathbf{k}) c_{\beta\nu}^*(\mathbf{k}' - \mathbf{q}) c_{\gamma\nu}(\mathbf{k}') \quad (7)$$

Dipole matrix elements can be obtained through:

$$\vec{\xi}_{\mu\nu}(\mathbf{k}) = \frac{-i\hbar}{m} \frac{\mathbf{p}_{\mu\nu}(\mathbf{k})}{\varepsilon_{\mu}(\mathbf{k}) - \varepsilon_{\nu}(\mathbf{k})}. \quad (8)$$

for $\mu \neq \nu$

Time-dependent interband polarization density:

$$\begin{aligned} \mathbf{P}(t) &= \frac{e}{L^2} \sum_{\mathbf{k}} \text{Tr} \left[\vec{\xi}(\mathbf{k}) \rho(\mathbf{k}, t) \right] \\ &= \frac{e}{L^2} \sum_{\mathbf{k} \lambda \lambda'} \vec{\xi}_{\lambda \lambda'}(\mathbf{k}) \rho_{\lambda' \lambda}(\mathbf{k}, t). \end{aligned} \quad (9)$$

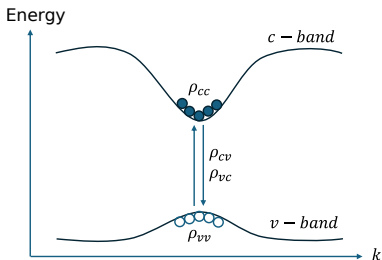


Figure: Density matrix element illustration

Numerical Evaluation of The Sum Over k-space

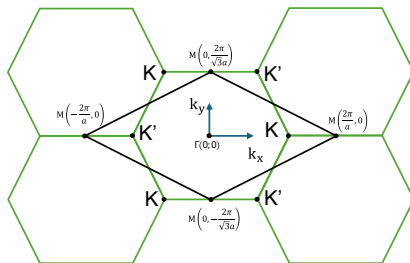
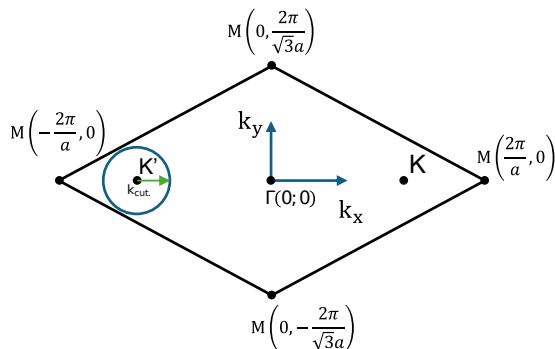


Figure: Rhombus primitive cell

$$\sum_{\mathbf{k}} \dots \rightarrow \frac{L^2}{4\pi^2} \int \int_{BZ} dk_x dk_y \dots \quad (10)$$

k-Cutoff



For k-points around K' point

$$W_{\mathbf{k}, \mathbf{k}', \mathbf{q}}^{\alpha\mu\beta\nu} \approx W_{\mathbf{k}, \mathbf{k}', \mathbf{q}}^{\alpha\mu\beta\nu} \theta(k_{cut.} - |\mathbf{k} - \mathbf{k}_{K'}|) \theta(k_{cut.} - |\mathbf{k}' - \mathbf{k}_{K'}|). \quad (11)$$

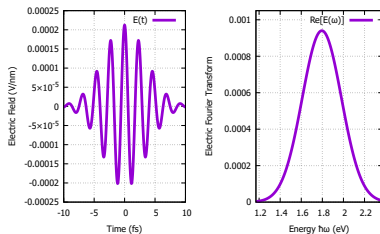
The same for k-points around K point

Electromagnetic Field

The electric field has a Gaussian envelope form:

$$\mathbf{E}(t) = \mathbf{E}_0 \cos(\omega_0 t) e^{-\frac{t^2}{\tau_L^2}} \quad (12)$$

- small E_0 : $\rho_{cc}(\mathbf{k}) \rightarrow 0$
- $\hbar\omega_0 = E_{gap}$.
- small $\tau_L \rightarrow$ rounder Fourier transform's peak around ω_0



Absorption coefficient²:

$$\alpha(\omega) \propto \frac{P(\omega)}{E(\omega)}. \quad (13)$$

²Haug and Koch, *Quantum Theory Of The Optical And Electronic Properties Of Semiconductors* (5th Edition).

- Two resonance labeled by A (1.93 eV) and B (2.1 eV) are exciton peaks (band split due to SOC)
- Weak trion peak near A labeled by A' (18 meV)

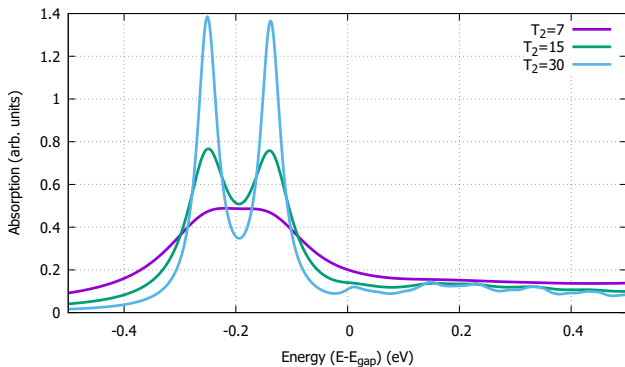
$$E_{gap} = 2.15 \pm 0.06 \text{ eV}$$

- Relative permittivity ϵ

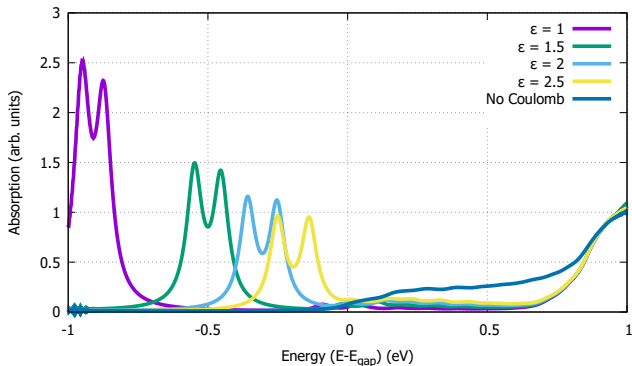
$$E_{bind.} = E_{gap} - E_A = 0.22 \text{ eV}$$

- Dephasing time T_2

◀ ◻ ▶ ◀ ◻ ▶ ◀ ≡ ▶ ◀ ≡ ▶ ≡ ▶ ↺ 🔍 ↻



- Choosing the T_2 for clearer Exciton peak.
- The bigger T_2 , the clearer main Exciton peaks \rightarrow confirm two peak.
- At $T_2 = 30$ fs show other smaller peaks \rightarrow predict other peaks.



- Choosing the ε for fitting with the experiment.
- For 3-band TB model: $\varepsilon \in (1.5, 2.5)$ is in good agreement with exciton binding energy of $E_{bind.} = 0.2 - 0.5\text{eV}$

Summary:

- From three-band TB + SBE \rightarrow Linear Absorption Spectrum
- We confirm the Exciton binding energy in this model is in agreement with experimental data, and predict smaller exciton peaks.

Further research:

- High Harmonic Generation
- High-order Side-band Generation
- Photovoltaic effect

Thank you for your listening.